goes transition. Thus, the entire shock structure collapses together, as noted by Muntz, Hamel and Maguire.[8] Hence, there is experimental confirmation of the present theory in this limit. However, further experiments are required over a wider range of Re^* in order to distinguish which rarefaction parameter (δ/R_{MD} or R_t/R_{MD}) properly describes the breakdown of the continuum theory. In order to experimentally verify the results illustrated in Fig. 3, proper simulation of the rocket plume must be achieved. Particular emphasis should be placed on obtaining the critical Reynolds number for the merging of the barrel shock. To the author's knowledge, no such experimental data have been published and Fig.3 is presented as a guideline to theoretical modeling of high-altitude rocket plumes.

References

[1] Albini, F. A., "Approximate Computation of Underexpanded Jet Structure," *AIAA Journal*, Vol. 3, No. 8, Aug. 1965, pp. 1535–1537.

[2] Hubbard, E. W., "Approximate Calculation of Highly Underexpanded Jets," *AIAA Journal*, Vol. 4, No. 10, Oct. 1966, pp. 1877–1879.

[3] Boynton, F. P., "Highly Underexpanded Jet Structure: Exact and Approximate Calculations," *AIAA Journal*, Vol. 5, No. 9, Sept. 1967, pp. 1703–1704.

[4] Ashkenas, H. and Sherman, F. S., "The Structure and Utilization of Supersonic Free Jets in Low Density Wind Tunnels," *Rarefied Gas Dynamics, Fourth Symposium*, Vol. II, Academic Press, New York, 1966, pp. 84–105.

[5] Hayes, W. D., and Probstein, R. F., *Hypersonic Flow Theory*, Academic Press, New York, 1959.

[6] Probstein, R. F., "Shock Wave and Flow Field Development in Hypersonic Re-entry," *ARS Journal*, Vol. 31, No. 2, Feb. 1961, pp. 185–194.

[7] Ahouse, D. R., and Bogdonoff, S. M., "An Experimental Flow Field Study of the Rarefied Blunt Body Problem," AIAA Paper 69-656, San Francisco, Calif., 1969.

[8] Muntz, E. P., Hamel, B. B., and Maguire, B. L., "Some Characteristics of Exhaust Plume Rarefaction," *AIAA Journal*, Vol. 8, No. 9, Sept. 1970, pp. 1651–1658.

[9] Bier, K., and Schmidt, B., "Zur Form der Verdichtungsstossen in Frei Expandierenden Gasstrahlen," *Zeitschrift Agnew Physik*, 13, 1961, pp. 493–500.

[10] Hamel, B. B., and Willis, D. R., "Kinetic Theory of Source Flow Expansion with Application to Free Jet," *The Physics of Fluids*, Vol. 9, No. 5, May 1966, pp. 829–841.

[11] Muntz, E. P., Hamel, B. B., and Maguire, B. L., "Exhaust Plume Rarefaction," AIAA Paper 69-657, San Francisco, Calif., 1969.

MARCH 1972 AIAA JOURNAL VOL. 10, NO. 3

Flowfield Interactions Induced by Underexpanded Exhaust Plumes

R. C. BOGER,* H. ROSENBAUM,† AND B. L. REEVES‡
Avco Systems Division, Wilmington, Mass.

Experiments have been conducted on a slender cone at Mach 10 with a highly underexpanded exhaust plume to determine the flowfield interactions, including the separation pattern and the influence upon aerodynamic coefficients. The experimental results show that the plume induces a preferential separation on the leeward side and that this can result in destabilizing aerodynamic forces. The experiments suggest a straightforward analytical model to predict the extent of separation on the cone and the reattachment of the separated boundary layer on the plume boundary. This model has been checked against the experimental results, and is used to predict the plume-induced separation pattern at angle of attack.

Nomenclature

A	= the base area of the cone
C_X, C_N, C_M	= axial force, normal force, and pitching moment
H, J, f, D	= integral functions used in the moment-integral method
L	= length of the sharp cone
M	= freestream Mach number
M_p	= inviscid Mach number along edge of constant pressure plateau region
p	= pressure
q	= freestream dynamic pressure
r	= radial distance on cone's base
R	= base radius of the cone
Re	= Reynolds number
u_e	= velocity along edge of separated flow region
u^*	= velocity along dividing streamline
x, y, z	= axial and normal body coordinates, Fig. 1
Δx	= distance downstream of separation
X	= transformed coordinate for separated shear layer
α	= angle of attack
δ_i^*	= transformed displacement thickness
ϕ	= meridional angle, Fig. 1
θ	= reattachment turning angle, Fig. 11
θ_c	= cone angle
θ_0	= boundary-layer momentum thickness at separation
θ_i	= transformed momentum thickness
Θ	= angle between local inviscid streamline entering the shear layer and inviscid stream direction downstream of the plume-shear layer interaction

Subscripts

ch	= plenum chamber conditions
cone	= cone value for attached flow
e	= value at edge of region of separated flow
sep	= separated flow value
s	= stagnation conditions behind a normal shock

Presented as Paper 71-562 at the AIAA 4th Fluid and Plasma Dynamics Conference, Palo Alto, June 21–23, 1971; submitted July 12, 1971; revision received November 1, 1971. This work was partially supported under Air Force Systems Command Contract F04701-68-C-0293. R. Haynes was the SAMSO Project Officer, and G. Friese of the Aerospace Corporation was the Project Engineer. The authors gratefully acknowledge the generous assistance of several of their coworkers at Avco Systems Division.

Index category: Jets, Wakes, and Viscid-Inviscid Interactions.

* Senior Staff Scientist. Associate Member AIAA.

† Senior Consulting Scientist. Member AIAA.

‡ Senior Consulting Scientist. Member AIAA.

Introduction

A SERIES of experiments has been conducted to study the flowfield interactions induced by a highly underexpanded plume, issuing from a sonic nozzle centered in the base of a 6° cone. The plume axis was parallel to the freestream at zero angle of attack. The results of the experiments, obtained from pressure measurements and optical coverage, yield information on the extent of separated flow over the cone, the destabilizing influence upon aerodynamic forces and moments, and the nature of the interaction between the external stream and the plume. By forming an obstacle to the flow, the plume in these experiments induced separation as far as halfway forward on the cone's surface at zero angle of attack.

Previous work on the problem[1-4] has demonstrated that large areas of separated flow can be induced on a body by the underexpanded plume. The change in the separation pattern with angle of attack was also noted. However, the body shapes tested were a cone-cylinder-flare and a blunted cylinder, so that the separation pattern was strongly influenced by these shapes.

More attention has been given to the interaction of a transverse jet with a supersonic stream.[5-7] This interaction acts as a fluid amplifier, which increases the side force of the jet and offers promise as a control device. It has been recognized, that the separated flow ahead of the jet may be considered similar to that caused by a forward-facing step, whose height is equivalent to the penetration height of the jet. When the plume is directed parallel to the stream, however, the penetration height criterion cannot be employed.

As the plenum pressure rises, the plume gradually fills out the near wake of the cone, and further increases in the plenum pressure cause the plume to extend beyond the cone's base, so that it begins to interfere with the conical flow. The base pressures increase simultaneously and eventually reach the value required to separate the flow on the cone. As long as separation does not extend to the nose of the cone, the base pressures are greater than the pressures over the cone's surface. When the pressures on the cone and its base are summed, the resulting pressure drag is found to be negative.

At angle of attack, separation moves forward on the leeward side and backward on the windward side, and the plume is slightly asymmetric as well. This circumstance can lead to higher pressures over the after portion of the leeward side. The pressures result in a force, acting behind the center of gravity, which drives the cone to larger angles of attack. At a sufficiently large angle of attack, the separated region on the leeward side extends nearly to the nose, and a static trim angle is achieved. The present results show trim angles close to the cone angle under certain conditions.

These experiments have led to a straightforward analysis of the entire interaction region, which predicts the extent of separation on the cone and the location of reattachment on the plume

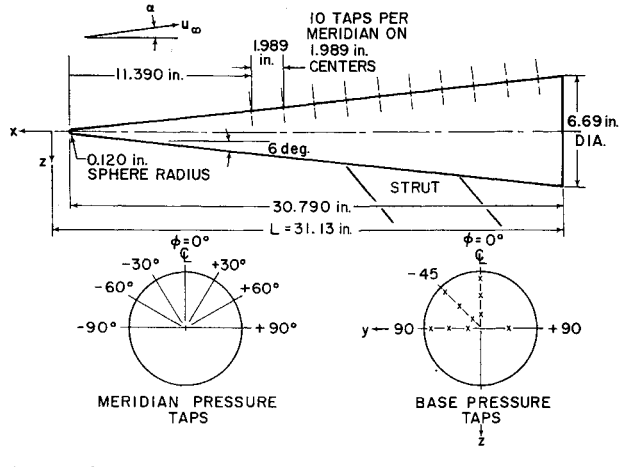

Fig. 1 Schematic of the experimental model and pressure tap locations.

Table 1 Test matrix

p_{ch}/p_∞	α, deg	Re/ft	M
0	0, 2, 4, 8	0.25×10^6	10
5678	0, 2, 4, 8	0.25×10^6	10
22,400	0, 2, 4, 8	0.25×10^6	10
55,250	0, 2, 4, 8	0.25×10^6	10
100,000	0	0.25×10^6	10
175,000	0, 2, 4, 8	0.25×10^6	10
21,000	0, 4	2.4×10^6	10

boundary. In this model the plume is assumed to expand inviscidly, forming an effective body, which if sufficiently large may induce separation upstream on the cone. The plume boundary is in turn dependent upon the pressure in the region of separated flow, and this pressure varies with Mach number, Reynolds number, and the length of separation. In order to determine a unique solution, the reattachment of the viscous shear layer must be compatible with the pressure rise occurring where the supersonic stream interior to the plume meets the one exterior to the region of separated flow. This solution is accomplished using a strong interaction, wakelike model of the separated shear layer impinging on the plume boundary. The approach developed here considers the detailed structure of the plume and differs somewhat from the situation treated by Klineberg, Kubota, and Lees.[8] The viscous shear layer along the plume boundary is neglected in the present analysis.

By assuming a two-dimensional strip interaction, this analysis can be applied to the body at small angle of attack. This has been checked against a specific experimental result, and it agrees with the measured separation pattern, pressures, and interactions. Consequently, the analysis can be employed to predict the possible destabilizing influence of the plume on the aerodynamic coefficients.

Description of the Experiment

The tests were conducted in Tunnel C of the von Kármán Gas Dynamics Facility, Arnold Engineering Development Center. This is a Mach 10 continuous flow 50-in. test-section wind tunnel. Most of the tests were run at a freestream Reynolds number per ft of 0.25×10^6, with two additional tests conducted at 2.4×10^6.

The model consisted of a 6° cone instrumented with 70 pressure taps on its surface and 10 on its base as shown in Fig. 1. Its base diameter is 6.69 in. The jet issued from a sonic nozzle of 0.477 in. diam located in the center of the cone's base. The plenum chamber in the conical model was supplied with pressurized air at ambient temperature through the supporting strut, and the plenum pressure was monitored during the tests. In order to avoid strut interference effects, the pressure taps were located on the top side of the cone opposite the strut. No interference was discernible in the tests. Angle-of-attack data were obtained by combining $+\alpha$ and $-\alpha$ results.

The size of the plume is governed by the ratio of plenum pressure to freestream static pressure, p_{ch}/p_∞. Six values of p_{ch}/p_∞ were used in the tests in addition to the no blowing case. The test matrix is shown in Table 1 with the angles of attack for each p_{ch}/p_∞.

Results of the Experiment

Increasing p_{ch}/p_∞ from the no blowing case, results in the plume gradually filling out the near wake region behind the cone. Figure 2 shows the shadowgraph for the case where $p_{ch}/p_\infty = 2.1 \times 10^4$, $Re_\infty/\text{ft} = 2.4 \times 10^6$, and $\alpha = 0$. The plume fills out the entire near wake region here, but has not yet induced separation on the cone. The features of the flowfield visible on this shadowgraph include the plume shock, the laminar (or possibly transitional) shear layer leaving the end of the cone, the interaction shocks which occur where the plume meets the external flow, and even the line of turbulence at reattachment.

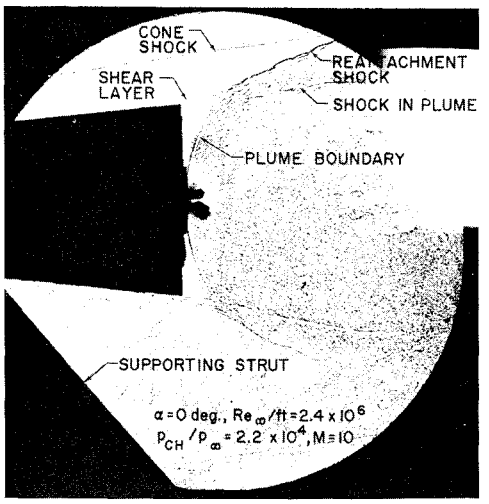

Fig. 2 Shadowgraph of plume interaction without separation on the cone.

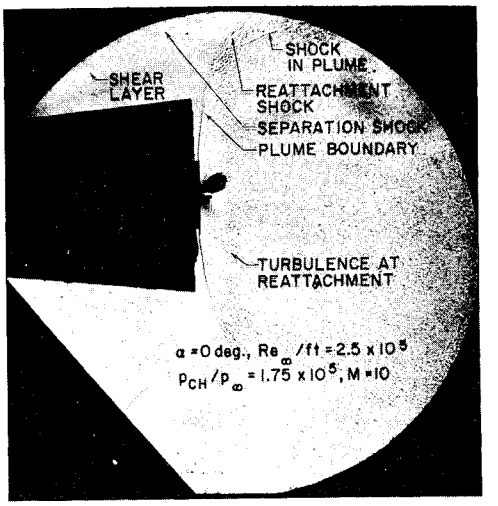

Fig. 4 Shadowgraph of plume induced separation on the cone.

The first occurrence of separation on the cone at $\alpha = 0$ and $Re_\infty/\text{ft} = 0.25 \times 10^6$ was for $p_{ch}/p_\infty = 5.5 \times 10^4$. The pressure distribution for this case is shown in Fig. 3. Note that the base pressures, plotted on the right-hand side of this figure, are close to the plateau pressure in the separated region. The largest value of p_{ch}/p_∞ attained in the experiment was 1.75×10^5, and the resulting plume caused separation to move about half-way up the cone at $\alpha = 0$. This is also shown in Fig. 3, where the plateau pressure is again seen to be uniform and equal to the base pressure. The shadowgraph of this case, Fig. 4, shows the large plume extending well beyond the cone's base, and the interaction where the laminar shear layer reattaches to the plume boundary.

At angles of attack, the flowfield about the cone is no longer symmetric. Separation moves forward on the leeward side and backward on the windward side. Figure 5 shows the pressure distributions on the windward, side, and leeward meridians when $\alpha = 2°$ for the case when $p_{ch}/p_\infty = 5.5 \times 10^4$. Comparison with Fig. 3 shows that separation has moved more than halfway up the cone on the leeward side, and has disappeared on the windward side. The base pressure is higher on the windward than on the leeward side. The pressures for $p_{ch}/p_\infty = 1.75 \times 10^5$ and $\alpha = 2°$ are shown in Fig. 6. The separation on the leeward side extends to $x/L = 0.32$ as verified by oil flow studies. For reference the no blowing result for $\alpha = 2°$ is given in Fig. 7.

Aerodynamic Coefficients

The pressure distribution, obtained from the 80 pressure taps, was integrated to obtain aerodynamic coefficients. In order to obtain the complete circumferential pressure distribution, the measurements were made at $\pm\alpha$ and then combined. On the cone's surface the pressure was measured at each of the 10 axial stations shown in Fig. 1 and at 14 circumferential points corresponding to $\phi = 0°, \pm 30°, \pm 60°, \pm 90°, \pm 120°, \pm 150°, 180°$. Note that there are actually 4 measurements at $\phi = \pm 90°$.

To work with these data, the measured pressures are first averaged at $\phi = \pm 30°$, etc. This is equivalent to assuming symmetry about the pitch plane. Then the circumferential distribution is fitted to a cosine series

$$p(x_i) = \sum_{n=0}^{6} P_n(x_i) \cos^n \phi, \qquad i = 1, \ldots, 10$$

The base pressure data are handled in a similar manner and fitted to a series in terms up to $\cos^4 \phi$. The resulting series are integrated over the surface and base of the cone to obtain the aerodynamic coefficients. The axial force coefficient is defined as

$$C_X = \frac{-2\tan^2\theta_c}{Aq} \int_0^L \int_0^\pi p \, d\phi x \, dx + \frac{2}{Aq} \int_0^R \int_0^\pi p \, d\phi r \, dr$$

the normal force coefficient is

$$C_N = \frac{-2\tan\theta_c}{Aq} \int_0^L \int_0^\pi p \cos\phi \, d\phi x \, dx$$

and the pitching moment coefficient about the nose is

$$C_{M_0} = \frac{-\tan\theta_c}{ARq\cos^2\theta_c} \int_0^L \int_0^\pi p \cos\phi \, d\phi x^2 \, dx + \frac{2}{ARq} \int_0^R \int_0^\pi p \cos\phi \, d\phi r^2 \, dr$$

The coordinate system used to define them is shown in Fig. 1.

At zero angle of attack the base pressure contribution to the

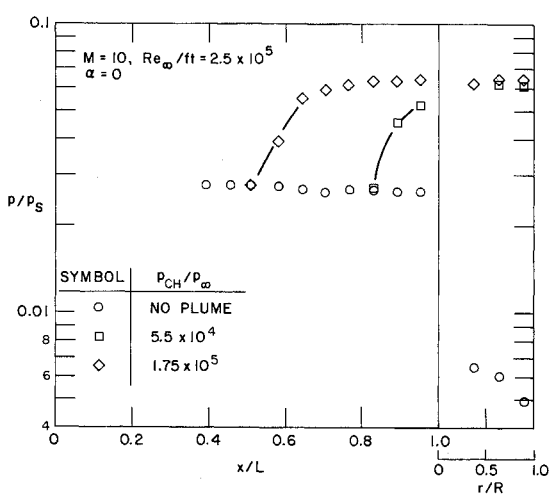

Fig. 3 Pressure distributions on the cone's surface and base at zero angle of attack.

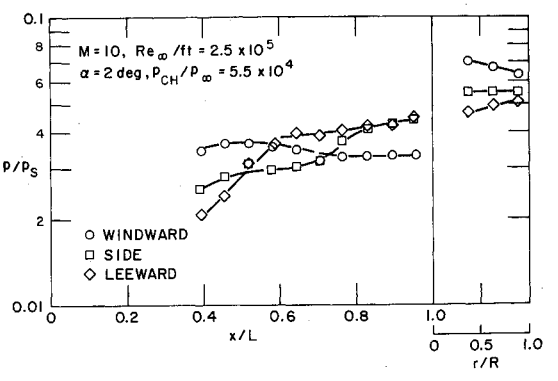

Fig. 5 Pressure distributions at angle of attack, $p_{ch}/p_\infty = 5.5 \times 10^4$.

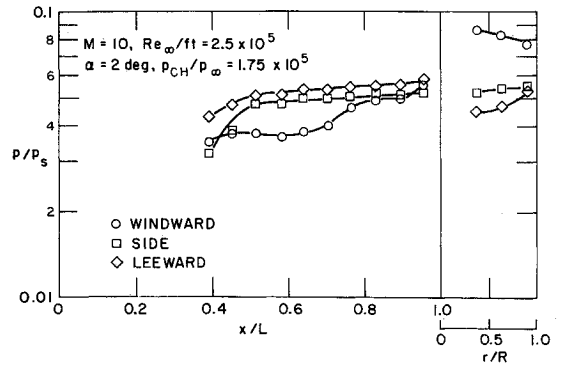

Fig. 6 Pressure distribution at angle of attack, $p_{ch}/p_\infty = 1.75 \times 10^5$.

axial force coefficient increases with increasing p_{ch}/p_∞ to a maximum as shown in Fig. 8. The maximum occurs when the base pressure equals the pressure needed to induce separation on the cone. For larger values of p_{ch}/p_∞ and larger plume sizes, separation moves forward on the cone, but the plateau pressure changes very little. The cone's contribution to the axial force begins at a negative value and decreases as separation moves up the cone. The total axial force coefficient is obtained from the sum of the base and cone contributions. The notable feature of this result is that the axial force changes sign.

The plume acts to increase the region of separated flow on the leeward side at angle of attack. As was shown in Fig. 5, this can lead to an attached flow on the entire windward side, while a higher pressure exists in the separated region on the leeward side. The resultant in this case is a destabilizing force. For a larger plume, separation begins on the windward side, while it moves still further forward on the leeward side, and the effect on aerodynamic coefficients is more complicated. The normal force coefficient, shown in Fig. 9, is reduced and even changes sign because of the plume. To demonstrate the influence on pitching moment, the center of gravity was assumed to be at $0.62L$, yielding a static margin of $0.05L$, based upon Newtonian theory. The resulting pitching moment coefficient with respect to this center of gravity is shown in Fig. 10. A stable pitching moment coefficient is negative using the present definition. The experimental results show that the plume leads to instability at small angles of attack, and a static trim angle in the vicinity of 6° is indicated.

Analysis of Flowfield Interactions

The shadowgraphs and pressure data obtained in these experiments have led to the development of an analytical model of the

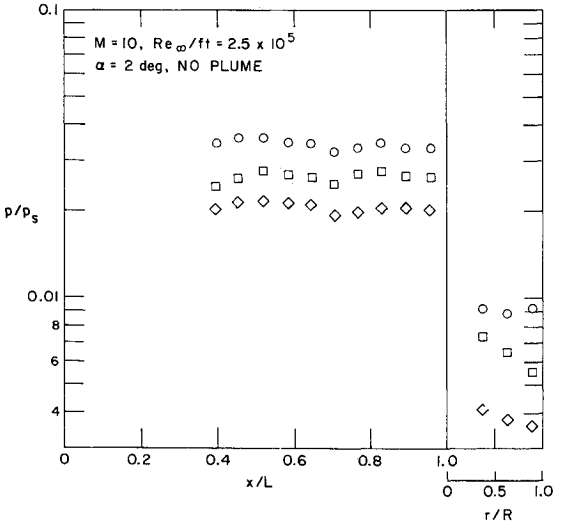

Fig. 7 Pressure distribution at angle of attack without a plume.

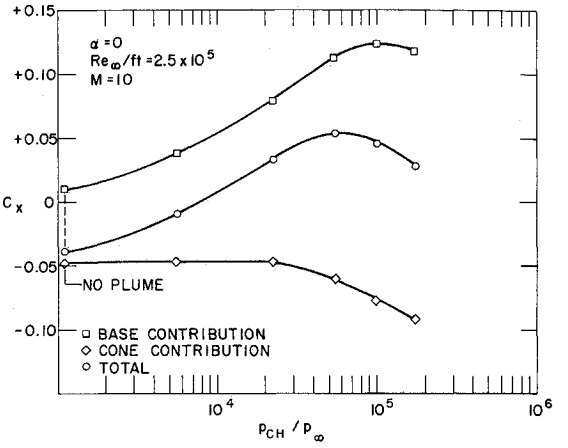

Fig. 8 Axial force.

entire interaction region. For these experiments, in which the laminar separated shear layer apparently was tripped by the strong compression at the "reattachment"§ point on the plume boundary, the extent of separation on the cone, the location of reattachment, and the reattachment turning angle θ (see Fig. 11) produced by the interaction of the plume with the shear layer are in generally good agreement with predictions resulting from this model. In the model the plume is assumed to expand inviscidly, forming an effective body, which may induce separation on the cone. The approach to be described is applicable given the Mach number, Reynolds number, body configuration, nozzle exit condition, and, of course, an empirical statement concerning the location of transition.

The behavior of the separating shear layer depends on whether it is laminar, transitional, or turbulent. Following Chapman, Kuehn, and Larson,[9] it is worthwhile noting the possible cases that can arise in strong plume interactions. Assume a specific, fixed configuration, freestream Mach number, and p_{ch}/p_∞. For a sufficiently low-freestream Reynolds number, transition occurs far enough downstream of the shear layer-plume impingement so that the interaction is purely laminar. The solution can be computed using the methods of Lees and Reeves[10] and Klineberg and Lees.[11]

As the Reynolds number is increased transition moves upstream and, evidently for sufficiently strong plumes, "sticks" at the reattachment point over a fairly large range of Reynolds numbers. This process is similar to the transition sticking phenomenon at the near wake stagnation point. Here, however, because of much stronger compressions at reattachment on the plume boundary, the sticking phenomenon is apparently even

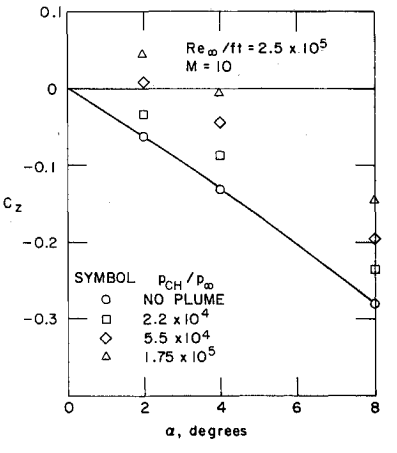

Fig. 9 Normal force.

§ The "reattachment" point is the point where the dividing streamlines of the separated shear layer and plume boundary meet. Consequently, it is a stagnation point.

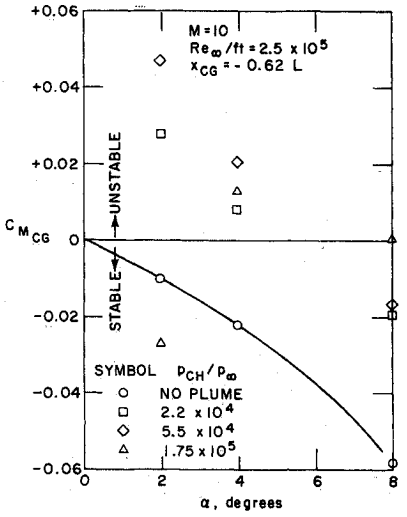

Fig. 10 Pitching moment.

more dramatic than in the near wake.¶ In the present experiments, in which the Mach number on the cone surface ahead of separation was 8.2, the separated shear layer was tripped at reattachment for values of $Re_{\Delta x}$ as low as 10^5! According to Chapman, Kuehn and Larson's[9] results, $Re_{\Delta x}$ for natural transition of the shear layer is about 10^6 at Mach 4, and their results show that $Re_{\Delta x}$ for natural transition increases with increasing Mach number. Consequently, it appears that for sufficiently strong plumes transition sticks at the reattachment point over *at least* a decade in Reynolds number.

Finally, as the Reynolds number is increased further transition moves upstream in the separated shear layer on the cone and eventually moves upstream of the separation point itself. For plume interactions in which the separated shear layer is fully turbulent the method given in Refs. 12 and 13 can be used to find the separation point and reattachment turning angle.

Since in all of the present experiments transition appeared to occur suddenly at the reattachment point, we have applied the general analyses of laminar[10,11] and turbulent[12,13] interactions to the special case of a laminar separated shear layer, followed by an instantaneous transition to turbulent flow and a turbulent reattaching shear layer.

The crucial simplifying assumption used in this model is that the plume expands inviscidly into the plateau pressure of the separated shear layer on the cone. This assumption has been verified in all of our experiments (see Figs. 3, 5, and 6) and it permits us to neglect the details of the inner shear layer along the plume boundary because inviscid plume shapes computed using the plateau pressure as the back pressure compare quite well with shapes obtained in shadowgraphs. It is plausible that this key assumption is also applicable to strong plume interactions that are purely laminar or fully turbulent (using, of course, the appropriate laminar or turbulent plateau pressure) but additional experiments are needed over a much wider range of Reynolds number to verify this. Because of this assumption, the flow model is limited to strong plumes in which a region of extensive separation and a constant pressure plateau is produced on the cone surface.

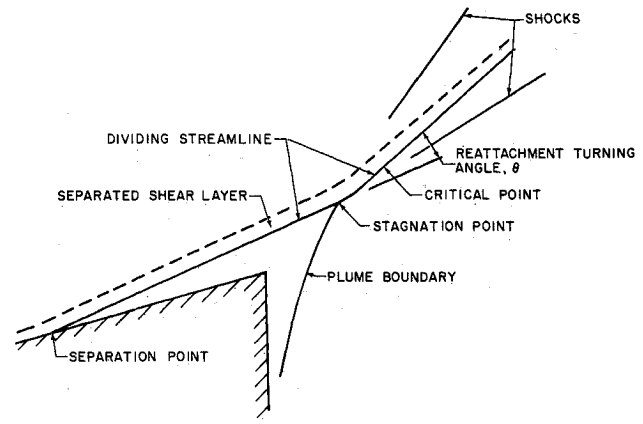

Fig. 11 Analytical model of the flowfield interactions.

In general, the four steps necessary for obtaining an iterative solution for plume interactions are as follows:

1) For an assumed separation point location the separation angle, plateau pressure, and Mach number M_p corresponding to the plateau pressure are determined. This also defines a preliminary impingement point on the plume boundary.

2) For the given M_p and the shear layer development the turning angle at reattachment is obtained from the viscous interaction solution. The shear layer development is the extent to which the velocity along the dividing streamline has approached the asymptotic value $\sim 0.6u_e$.

3) From inviscid (method-of-characteristics) plume calculations the pressure and Mach number along the plume boundary and its location are known. By solving for the deflection of the two supersonic stream internal and external to the plume, the impingement point on the plume boundary resulting in the desired turning angle of the external stream is found.

4) The impingement point determined from 3 is compared with that in 1. A new separation point compatible with 3 is chosen and the four steps are repeated.

As a specific example we have treated the case of $p_{ch}/p_\infty = 1.75 \times 10^5$ and $\alpha = 0$, which was shown in Figs. 3 and 4. The flow is idealized as a laminar separated and a turbulent reattaching shear layer. The value of the plateau pressure is accurately predicted** using the relationship for laminar separated flow,[14]

$$p_{sep}/p_{cone} = 1 + 1.20\, M_{cone}^{3/2} Re_{X_{sep}}^{-1/4}$$

The experimental point of separation is used here. The Mach number along the edge of the separated flow, in the pressure plateau region M_p is 7.45, and the separation angle with respect to the cone is 4°.

Downstream of separation, the normalized velocity on the dividing streamline u^*/u_e grows as a function of $X^2/\theta_0^2 Re_X$, where X is the transformed distance downstream of separation and θ_0 is the boundary-layer momentum thickness at separation. This

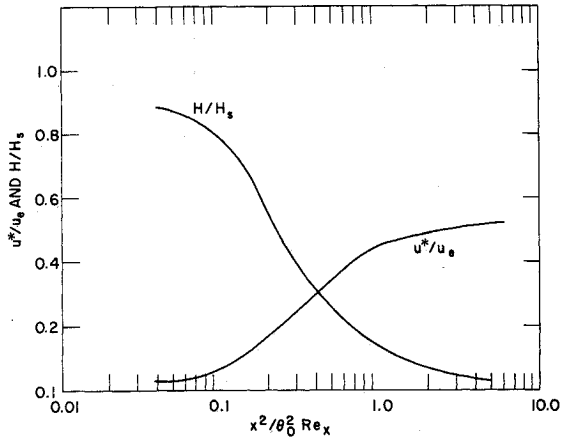

Fig. 12 Laminar separated flow solutions.

¶ Clearly, for a given Reynolds number the strength of the plume interaction p_{ch}/p_∞ also plays a role in determining the location of transition. Increasing this parameter not only increases the length of separation (and thus increases $Re_{\Delta x}$, where Δx is the distance from the separation point to the reattachment point) but also increases the compression at reattachment, which can trip the shear layer.

** In agreement with the analysis of laminar interactions in Refs. 10 and 11.

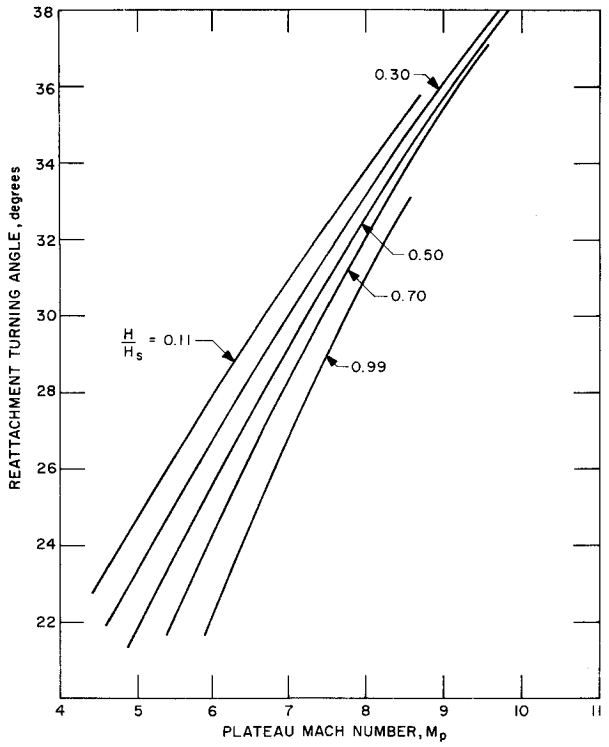

Fig. 13 Turbulent reattachment solutions.

shear layer development, obtained from Ref. 15, is given in Fig. 12. In discussing the reattachment solution, it is more convenient to work with an alternate parameter H/H_s. The relationship between u^*/u_e and H/H_s is determined by the Cohen and Reshotko family of laminar similar solutions for reverse flow[10] and is given in Fig. 12.

As pointed out in Ref. 9, the character of the separated flowfield depends upon the location of transition. In the present situation, examination of the shadowgraph reveals that transition appears just as the shear layer reattaches to the plume boundary. On this basis, the reattachment solution was computed as a fully turbulent wakelike flow, as formulated in Refs. 12 and 13. In this model the viscous-inviscid interaction is computed using the moment integral method, and it determines the turning angle of the reattaching shear layer. The integral equations of continuity, momentum and first velocity moment are respectively, for $\partial p/\partial y = 0$ (Refs. 12 and 13)

$$\left[H + \left(\frac{1+m_e}{m_e}\right)\right]\frac{d\delta_i^*}{dX} + \delta_i^*\frac{dH}{dX} + f\frac{\delta_i^*}{M_e}\frac{dM_e}{dX} = \frac{\tan\Theta}{m_e} \quad (1)$$

$$H\,d\delta_i^*/dX + \delta_i^*\,dH/dX + (2H+1)(\delta_i^*/M_e)\,dM_e/dX \simeq 0 \quad (2)$$

$$J\,d\delta_i^*/dX + \delta_i^*\,dJ/dX + (3J\delta_i^*/M_e)\,dM_e/dX = D \quad (3)$$

where H, J, f, and D are one-parameter integral functions for separated, wakelike flows defined in Refs. 12 and 13, δ_i^* is a transformed displacement thickness, X is the transformed coordinate measured along the plume boundary, and $\Theta(X)$ is the angle between the local inviscid streamline entering the shear layer at any point X and the inviscid streamline direction at the edge of the shear layer downstream of the plume-shear layer interaction. In these solutions the two-dimensional Prandtl-Meyer relation was used to relate the inviscid stream inclination to the local edge Mach number M_e even though the flow is axisymmetric (or three-dimensional if the body is at angle of attack). For turbulent reatttachment and large plumes, that is for plumes larger than the base radius, the length scale of the compression is much smaller than the plume radius. Thus, the change in the streamline metric in this region is also small and has a negligible effect on the interaction.

The integral equations are solved by specifying the value of H/H_s and the Mach number at the beginning of reattachment (plateau Mach number). These are two of the three initial conditions required for the solution of Eqs. (1–3). By introducing the nondimensional variables $\tilde{\delta}_i^* \equiv \delta_i^*/(\delta_i^*)_0$ and $\tilde{X} \equiv X/(\delta_i^*)_0$, where $(\delta_i^*)_0$ is the transformed displacement thickness at the beginning of the compression at reattachment, Eqs. (1–3) are solved subject to the third initial condition: $\tilde{\delta}_i^* = 1$. The value of Θ at the beginning of reattachment is determined by the unique integral curve (say M_e vs X) passing through the critical point, which is located just downstream of the reattachment (stagnation) point. This solution is obtained by iterating on an assumed value of Θ at the beginning of reattachment.[12] Because the subcritical reattaching flow upstream of the critical point is independent of the supercritical flow downstream of the critical point, the turning angle at reattachment θ can be found without considering details of the merged shear layers from the body and plume downstream of the critical point. For a wakelike model of turbulent reattachment, the solution is independent of Reynolds number.

For turbulent reattachment the turning angle depends on M_p and the parameter H/H_s, which determines the extent to which the separated boundary layer has relaxed toward a free shear layer. To join the turbulent reattachment solution to the laminar shear layer, we assumed that $(H/H_s)_{\text{laminar}} = (H/H_s)_{\text{turbulent}}$ across the transition region, i.e., that the velocity along the dividing streamline at transition is continuous. Thus, H/H_s at the beginning of the turbulent reattachment is determined by the laminar shear layer development as discussed previously. The specific results for the turning angle at turbulent reattachment as a function of M_p and H/H_s, are presented in Fig. 13. In the present case, $M_p = 7.45$ and $H/H_s = 0.11$, indicating that the separated boundary layer has nearly relaxed to a free shear layer. The predicted turning angle at reattachment is 32.3°.

As has been pointed out, the plume is assumed to expand into the separated flow plateau pressure. The calculation is effected through a method-of-characteristics solution using a constant pressure boundary condition. The results of the numerical calculations agree with the shape of the plume boundary in Fig. 4, up to the point of interaction with the free shear layer. At this point the supersonic stream external to the region of separated flow meets the supersonic stream of the expanding plume gas. The result of this interaction is two shock waves and an interjacent slip line. This pattern is uniquely determined by the requirements of pressure balance across the slip line and velocities parallel to it. For the case at hand the slip line (the dividing streamline) is found to have an inclination of 42° with respect to the horizontal. This corresponds to a turning angle at reattachment of 32° for the separated shear layer, which is in close agreement with the predicted value of 32.3°. Furthermore, the reattachment shock is calculated to be 52°, and this agrees with the shock angle measured on the shadowgraph. Hence the essential features of the separated flow and its interaction with the plume, obtained from the analytical model, agree with this specific experiment at zero angle of attack.

The analytical model is most useful, however, at angle of attack in order to predict the pattern of separated flow and the consequent normal force and pitching moment coefficients. To apply the analysis on a body at angle of attack, a two-dimensional strip interaction is assumed. This implies that at each meridional

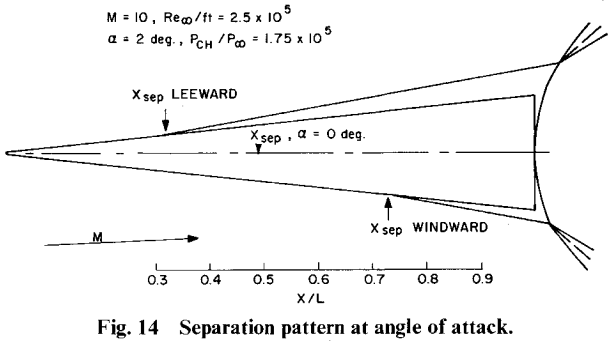

Fig. 14 Separation pattern at angle of attack.

station around the body, the local characteristics of the boundary layer are used to define separation. Also, a two-dimensional analysis of the shear layer growth and reattachment, and of the plume structure is employed.

The present analysis was applied to the same flow situation just analyzed, but with $\alpha = 2°$. For this situation, the separation on the windward side moves back to $x/L = 0.73$, while the leeward separation point is at $x/L = 0.32$, as shown in Fig. 14. It may be recalled that separation occurred at $x/L = 0.51$ for $\alpha = 0°$. The change in separation pattern with angle of attack is caused by the sensitivity of the plume to pressure changes along its boundary. On the leeward side, the plume expands in response to the lower separated plateau pressure, and in so doing forces the separation point further toward the nose. The results of the analysis, performed on the windward and leeward meridians, gave these separation points, matched the experimental pressures, and duplicated the interactions shown on the shadowgraph of this case. Therefore, the complete separated flowfield at angle of attack was determined analytically, and the unusual aerodynamic coefficients obtained experimentally can be predicted. The limitation on this two-dimensional strip interaction is that at large angles of attack crossflow effects become important. A similar limitation applies for the "tangent-body-technique," employed to calculate attached flows on slender bodies at angle of attack. That technique is known to have shortcomings when the angle of attack approaches the cone angle.

Conclusions

A series of experiments have been conducted to determine the flowfield interactions induced by a plume issuing from a sonic nozzle centered in the base of a 6° cone in a Mach 10 stream. The experiments have shown that the underexpanded plume interacts with the external stream to cause separation on the cone; and the separation pattern at angle of attack extends further on the leeward side than on the windward. When the pressure distributions over the body are integrated, the plume is found to have a destabilizing effect, and the high-base pressures produce a negative pressure drag or axial force.

These experimental results have led to the development of a straightforward analytical model of the entire interaction region that predicts the extent of separation and the location of reattachment on the plume boundary. The plume is assumed to expand inviscidly, forming an effective body, which may induce separation on the cone. The analysis has also been applied at angle of attack by using a two-dimensional strip interaction. The results of the analysis are checked with specific experimental results, and they show good agreement. This straightforward approach predicts the pattern of separated flow at angle of attack and the consequent aerodynamic coefficients.

References

[1] Alpinieri, L. J. and Adams, R. H., "Flow Separation Due to Jet Pluming," *AIAA Journal*, Vol. 4, No. 10, Oct. 1966, pp. 1865–1866.

[2] Flanga, R. A., Hinson, W. F., and Crawford, D. H., "Exploratory Tests on the Effects of Jet Plumes on the Flow over Cone-Cylinder-Flare Bodies," TN D-1000, Feb. 1962, NASA.

[3] Salmi, R. J., "Effects of Jet Billowing on Stability of Missile-Type Bodies at Mach 3.85," TN D-284, June 1960, NASA.

[4] McGhee, R. J., "Jet-Plume Induced Flow Separation on Axisymmetric Bodies at Mach Numbers of 3.00, 4.50, and 6.00," TM X-2059, Aug. 1970, NASA.

[5] Simpkins, P. G., "Secondary Mass Injection in a Hypersonic Flow," *Aeronautical Quarterly*, Vol. 22, Feb. 1971, pp. 53–64.

[6] Spaid, F. W. and Zukoski, E. E., "Study of the Interaction of Gaseous Jet from Transverse Slots with Supersonic External Streams," *AIAA Journal*, Vol. 6, No. 2, Feb. 1968, pp. 205–212.

[7] Sterrett, J. R. and Barber, J. B., "A Theoretical and Experimental Investigation of Secondary Jets in a Mach 6 Freestream with Emphasis on the Structure of the Jet and Separation Ahead of the Jet," *Separated Flows*, Pt. II, AGARD Conference Proceedings, No. 4, May 1966.

[8] Klineberg, J., Kubota, T., and Lees, L., "Theory of Exhaust-Plume/Boundary-Layer Interactions at Supersonic Speeds," AIAA Paper 70–230, New York, 1970.

[9] Chapman, D. R., Kuehn, D. M., and Larson, H. K., "Investigation of Separated Flows in Supersonic and Subsonic Streams with Emphasis on the Effect of Transition," TR 1356, 1958, NACA.

[10] Lees, L. and Reeves, B. L., "Supersonic Separated and Reattaching Laminar Flows: I. General Theory and Application to Adiabatic Boundary-Layer/Shock-Wave Interactions," *AIAA Journal*, Vol. 2, No. 11, Nov. 1964, pp. 1907–1920.

[11] Klineberg, J. M. and Lees, L., "Theory of Laminar Viscous-Inviscid Interactions in Supersonic Flow," *AIAA Journal*, Vol. 7, No. 12, Dec. 1969, pp. 2211–2221.

[12] Todisco, A. and Reeves, B. L., "Turbulent Boundary Layer Separation and Reattachment at Supersonic and Hypersonic Speeds," *Proceedings of Symposium on Viscous Interaction Phenomena in Supersonic and Hypersonic Flow*, 1969, University of Dayton Press, Dayton, Ohio, pp. 139–179.

[13] Hunter, L. G., Jr., and Reeves, B. L., "Results of a Strong Interaction, Wake-Like Model of Supersonic Separated and Reattaching Turbulent Flows," *AIAA Journal*, Vol. 9, No. 4, April 1971, pp. 703–711.

[14] Lewis, J., Kubota, T., and Lees, L., "Experimental Investigation of Supersonic Laminar Two-Dimensional Boundary-Layer Separation in a Compression Corner with and without Cooling," *AIAA Journal*, Vol. 6, No. 1, Jan. 1968, pp. 7–14.

[15] Reeves, B. L. and Lees, L., "Theory of Laminar Near Wake of Blunt Bodies in Hypersonic Flow," *AIAA Journal*, Vol. 3, No. 11, Nov. 1965, pp. 2061–2074.